



Rock glacier distribution across the Himalaya



Stephan Harrison ^{a,*}, Darren B. Jones ^a, Adina E. Racoviteanu ^b, Karen Anderson ^c, Sarah Shannon ^d, Richard A. Betts ^{e,f}, Ruolin Leng ^c

^a Faculty of Environment, Science and Economy, University of Exeter, Penryn Campus, Penryn, Cornwall TR10 9EZ, UK

^b Université Grenoble Alpes, CNRS, IRD, IGE – 38400 Saint Martin d'Hères, France

^c Environment and Sustainability Institute, University of Exeter, Penryn Campus, Penryn, Cornwall TR10 9EZ, UK

^d Bristol Glaciology Centre, Department of Geographical Science, University Road, University of Bristol, BS8 1SS, UK

^e Global Systems Institute, University of Exeter, Streatham Campus, Exeter EX4 4QE, UK

^f Met Office, FitzRoy Road, Exeter, Devon EX1 3PB, UK

ARTICLE INFO

Editor: Dr. Jed O Kaplan

Keywords:

Himalaya
Rock glaciers
Climate change
Water supplies

ABSTRACT

In High Mountain Asia, human-induced climate warming threatens the cryosphere. Expected long-term reductions in future runoff from glacial catchments raises concerns regarding the sustainability of these natural 'water towers' and the implications of reduced water availability for regional human and ecological systems. Ice-debris landforms (I-DL), containing ice whether moving or not include rock glaciers and ice-cored moraines, and are likely to be climatically more resilient than debris-covered and debris-free glaciers. Recent work has shown that rock glaciers contain globally valuable water supplies yet over High Mountain Asia information regarding their number, spatial distribution, morphometric characteristics and water content are scarce. Here, we present the first systematic estimate of the current extent and distribution of rock glaciers for a subset of High Mountain Asia (the Himalaya). A sample of 2070 intact and relict rock glaciers were digitized on Google Earth imagery from the Western, Central and Eastern Himalaya regions and then quantitative and qualitative characteristics were analysed regionally based on topographic data from the NASA Shuttle Radar Topography Mission (SRTM) Version 3.0 and then aggregated across the Himalaya using an "upscaling" method. The majority of the digitized landforms (~65%) were categorised as intact rock glaciers (i.e., ice-debris Landforms, or I-DLs, containing ice) and the remainder as relict rock glaciers (i.e., discrete debris accumulations or DDAs, not containing ice). They range in elevation from 3225 to 5766 m a.s.l., with the lowest in the Central Himalaya. Sampled relict and intact rock glaciers are primarily situated on northern quadrants. Over the entire Himalaya, we identified ~25,000 landforms, with a total estimated areal coverage of 3747 km². The area upscaling method was validated in the Manaslu region of Nepal using high-resolution Planet data (5 m) and freely available, fine spatial resolution optical satellite data accessed through Google Earth Pro and ESRI basemaps. In absence of complete rock glacier inventories over the Himalaya, our approach proves useful to investigate the nature, distribution and infer potential future behaviour of these landforms across the Himalaya in a changing climate.

1. Introduction

In High Mountain Asia (HMA), the cryosphere forms natural water towers that are integral for ecosystem services provision, and supplying multiple societal needs to ~800 million people living in the mountains and surrounding lowlands (Pritchard, 2019). However, considerable glacier mass loss has been documented in the last decades and is projected to continue throughout the twenty-first century and at an

accelerated pace (Kraaijenbrink et al., 2017; Hock et al., 2019; Maurer et al., 2019; Shannon et al., 2019) contributing to reduced water security and sea level rise (Caretta et al., 2022; Fox-Kemper et al., 2021). At smaller scales, an overall decrease in snow water equivalent (the quantity of water contained in a snowpack) has been reported for a number of catchments in the Himalaya, particularly during the pre-monsoon (March, April, May) and monsoon seasons (June, July, August) (Smith and Bookhagen, 2018). The continued decline of parts of

* Corresponding author.

E-mail addresses: Stephan.Harrison@exeter.ac.uk (S. Harrison), Adina.Racoviteanu@univ-grenoble-alpes.fr (A.E. Racoviteanu), Karen.Anderson@exeter.ac.uk (K. Anderson), Sarah.shannon@bristol.ac.uk (S. Shannon), R.A.Betts@exeter.ac.uk (R.A. Betts), rl552@exeter.ac.uk (R. Leng).

the Himalayan cryosphere raises major concerns for the future sustainability of water resources, particularly with regards to 'peak water' (the maximum glacier runoff reached before it starts to decline) (Huss and Hock, 2018; Immerzeel et al., 2020; Harrison et al., 2021). Indeed, even under the RCP4.5 climate modelling scenario, which represents emissions lower than expected with currently implemented policies, most basins fed by Himalayan glaciers are projected to reach peak water by ~2050, with the Indus reaching this at 2045 ± 17 years, the Ganges at 2044 ± 21 years and the Brahmaputra at 2049 ± 18 years (Huss and Hock, 2018).

Given the likely future decline in glacier runoff and the need for strong climate adaptation in HMA, it is important that the picture of available cryospheric water availability be complete. This requires a comprehensive, regional-scale understanding of all components of the hydrological cycle in the high-mountain cryosphere, beyond current estimates which account primarily for clean ice glaciers and to a smaller extent debris-covered glaciers (Immerzeel et al., 2012; Lutz et al., 2014; Kraaijenbrink et al., 2017; Huss and Hock, 2018; Zhang et al., 2019; Immerzeel et al., 2020). With continued climatically-driven glacier recession and mass loss, the relative hydrological value of rock glaciers in mountain regions is likely to become increasingly important since these features typically persist at elevations lower than glaciers and are insulated from warming by thick rock debris cover. Owing to the insulating and damping properties of the thick debris cover, rock glaciers are thought to be climatically more resilient than clean-ice and debris-covered ice glaciers where debris thickness often varies from several centimetres to a few meters at the terminus; consequently, their relative hydrological importance compared to that of debris-covered and debris-free glaciers may increase under future climate warming (Harrison et al., 2021). While rock glaciers may be more resilient to climate change, some studies show that rock glaciers have also accelerated and destabilised in the last two decades as a result of increasing temperatures (Delaloye et al., 2008; Marcer et al., 2021b). Yet, to date, with a few notable exceptions (e.g., Jones et al., 2019; Schaffer et al., 2019), the hydrological role of rock glaciers in HMA has received little consideration compared to both clean ice glaciers (see Fountain and Walder, 1998; Jansson et al., 2003; Irvine-Fynn et al., 2011; Huss and Hock, 2018) and debris-covered glaciers (Fyffe et al., 2019, and references therein; Miles et al., 2020; Miles et al., 2021).

Research suggests that rock glaciers may constitute increasingly important long-term water stores (Jones et al., 2018a), yet these are largely omitted from current water projections in HMA, because until now there has been no systematic reporting of their spatial distribution across the region. This prevents the understanding of their contributions to current and/or future water supplies across the wider region. Due to their morphological characteristic and complex structure, rock glaciers are difficult to delineate both in the field (also due to their remoteness, poor access and chaotic topography) and by remote sensing due to their spectral similarity with the surrounding terrain.

Rock glaciers have often been delimited using standard geomorphologic and kinematic approaches, i.e. using manual interpretation of aerial photography, optical images and/or interferometric synthetic aperture radar (InSAR) techniques combined with topographic data (Falaschi et al., 2014; Rangecroft et al., 2014; Robson et al., 2020; Cai et al., 2021; Buckel et al., 2022), but such methods are time consuming and require a-priori expert knowledge. New methods include the use of machine learning techniques to automate the mapping of rock glaciers (Robson et al., 2020; Wagner et al., 2020; Marcer et al., 2021a; Reinosch et al., 2021; Erharter et al., 2022). Most inventories remain regional in extent and are not yet applied at mountain-range scales (although see for example Erharter et al., 2022). However, while standard guidelines for inventorying rock glaciers have been established by the International Permafrost Association (IPA) Action Group (RGIK, 2022), significant work remains to produce rock glacier inventories for the globe. The spatial distribution and characteristics of rock glaciers is not included in global glacier inventories such as the Randolph Glacier Inventory (RGI)

and the Global Land Ice Monitoring from Space (GLIMS) database (www.glims.org). Furthermore, while systematic rock glacier inventory coverage has increased globally (Scotti et al., 2013; Falaschi et al., 2014; Rangecroft et al., 2014; Schmid et al., 2015; Marcer et al., 2017; Onaca et al., 2017; Wagner et al., 2020; Hassan et al., 2021; Reinosch et al., 2021), the Himalayan region is comparatively data-deficient (Jones et al., 2018a) although more recent assessments have been carried out (e.g. Chakravarti et al., 2022; Zhang et al., 2022). Indeed, Bolch et al. (2019) synthesised and evaluated the state of current scientific knowledge regarding changes in the high-mountain cryosphere, but rock glaciers received only a brief mention. Across HMA, with few exceptions (Jones et al., 2018b; Baral et al., 2019; Blöthe et al., 2019), rock glacier inventories have been conducted at relatively small spatial scales or are not spatially explicit (e.g., Regmi, 2008; Bolch and Gorbunov, 2014; Schmid et al., 2015); therefore, rock glacier distribution and their hydrological value are generally unknown.

Given the enormous spatial extent of HMA, manual digitization of rock glaciers is time consuming and subjective. In a previous study (Jones et al., 2018b), we developed a methodology to estimate the rock glacier extent for the Nepalese Himalaya by upscaling rock glaciers manually digitized from high-resolution satellite imagery in Google Earth based on surface characteristics (frontal and lateral margins, steep frontal slopes and ridge and furrow topography) (RGIK, 2022). Their likely hydrological importance was assessed in Jones et al. (2021). In this paper, we build upon this methodology presented in Jones et al. (2018b) to investigate the distribution of rock glaciers across the entire Himalaya. To our knowledge, this is the first comprehensive systematic estimate of rock glacier cover over this region. Our aim here is to validate the methodology presented in Jones et al. (2018a, 2018b) and use this approach to investigate the nature, distribution and potential future behaviour of these landforms across the Himalaya. These are required before we can determine their state and fate in a changing climate. We subdivide the rock glaciers into the following two broad categories. First, intact rock glaciers are those which we judge contain ice (whether or not they are moving). Second, relict rock glaciers are those which do not contain ice and do not display the characteristics of movement. This classification is discussed further in 3.2.

2. Study area

Our study area is the Himalaya, spanning ~ 1500 km in width (~ 76 to 92° longitude and ~ 26 to 34° latitude) (Fig. 1). To examine and highlight regional differences in the occurrence of rock glaciers, we use

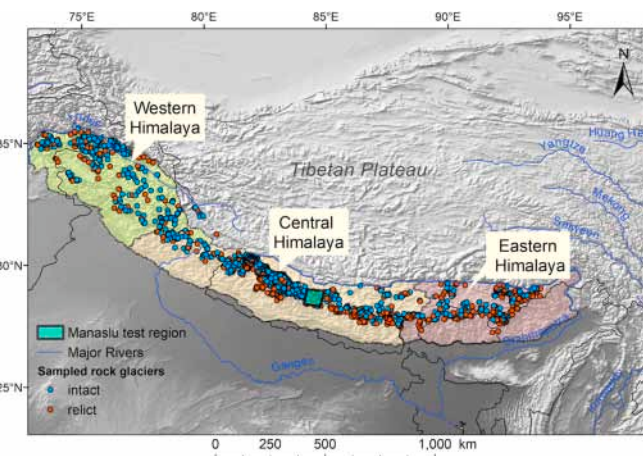


Fig. 1. Study area - the Himalaya - showing the three regions studied based on Bolch et al. (2012) and the distribution of sampled intact and relict rock glaciers. The major river systems are also shown: Amu Darya, Indus, Ganges, Brahmaputra, Salween, Mekong, Yangtze, and Irrawaddy. Also shown is the location of the Manaslu region in Nepal, used for validation.

three sub-regions selected across monsoonal gradients as defined in the literature (Bolch et al., 2012): Western Himalaya, Central Himalaya and Eastern Himalaya (Fig. 1). Climate in this region varies from dry, monsoon shadow in the west (Thayyen and Gergan, 2010) to wet, monsoon-influenced in the east (Barros and Lang, 2003; Bookhagen and Burbank, 2006).

For the independent validation of the inventory and an in-depth analysis of the rock glacier distribution, we focus on a subset area of the Himalaya domain centred on the Manaslu region (4704 km^2) located in the Central Nepal Himalaya. This region is situated in the headwaters of the Dudh Khola in the Manang district, Gandaki Province of Nepal (Fig. 1), at the climatic boundary between the regions affected by the Indian summer monsoon and those dominated climatically by the drier areas of the Tibetan plateau. The region comprises a mix of clean glaciers, debris-covered glaciers (Robson et al., 2018; Racoviteanu et al., 2022a) as well as rock glaciers; the latter have not been studied so far in this area. We chose this area due to the wealth of satellite imagery, including high-resolution Planet imagery from 2019 used in Racoviteanu et al., 2022a, and field reconnaissance during previous fieldwork (Racoviteanu et al., 2022a).

3. Methods

3.1. Data sources

In this paper we rely on freely available, fine spatial resolution optical satellite data accessed through Google Earth Pro and ESRI base-maps, including SPOT and DigitalGlobe (e.g. QuickBird, Worldview-1 and 2 and IKONOS) combined with topographic data from the NASA Shuttle Radar Topography Mission (SRTM) Version 3.0 Global 1 arc sec ($\sim 30 \text{ m}$) dataset (NASA-JPL, 2013). Google Earth was used to identify and “pin” rock glaciers across the Himalaya based on their surface characteristics. The SRTM DEM was used to calculate the slope of the terrain, which was then used as auxiliary data in the rock glacier delineation process. For the Manaslu region, we obtained a high-resolution satellite image (5 m) from Planet’s RapidEye constellation from November 2019, consisting of multispectral data (five spectral bands in the visible and near infrared) with a positional accuracy of $< 10 \text{ m}$ (Planet Labs, 2021). We used Level 3 A data, which consist of stripes comprising multispectral, radiometrically corrected orthorectified tiles with surface reflectance computed from top-of-atmosphere radiance products processed using the 6S radiative transfer model (Vermote et al., 1997) and MODIS data, which accounts for atmospheric effects (Planet Labs, 2021). We mosaicked these using nearest neighbour resampling technique to obtain a single image covering the Manaslu domain shown in Fig. 1. This was used for rock glacier delineation in conjunction with world imagery from the ArcGIS online base map (Sources: Esri, DigitalGlobe, GeoEye, i-cubed, USDA FSA, USGS, AEX, Getmapping, Aerogrid, IGN, IGP, swisstopo, and the GIS User Community) (see Section 3.4).

3.2. Rock glacier digitization and creation of the rock glacier sub-sample

For the systematic rock glacier inventory, we used manual feature identification and digitisation using geomorphic indicators for the Himalaya used in previous studies elsewhere (Baroni et al., 2004; Falaschi et al., 2014; Rangecroft et al., 2014) Table 1. Rock glaciers are generally identified based on their lobate or tongue-shaped landforms comprising a continuous, thick cover of rock debris overlying ice-supersaturated debris and/or pure ice, which creep slowly downslope (see Martin and Whalley, 1987; Barsch, 1996; Haeberli et al., 2006; Berthling, 2011) (Fig. 2a-b). The dynamic status of rock glaciers identified on the satellite imagery was assigned based on their presumed ice content and movement, according to the morphological classification by Barsch (1996) and established using geomorphic indicators (see Table 1 and Fig. 2a and b). The sampled landforms were classified based on their

Table 1

Geomorphic indicators used to identify rock glaciers and their activity status.

Geomorphic indicator	Intact rock glacier	Relict rock glacier
Surface flow structure	Well-defined furrow and ridge topography (Kääb and Weber, 2004)	Less defined furrow and ridge topography (Kääb and Weber, 2004)
Rock glacier body	Swollen body (Baroni et al., 2004). Surface ice exposures (Potter et al., 1998)	Flattened body (Baroni et al., 2004). Surface collapse features (Janke and Bolch, 2021)
Frontal slope	Steep (30–35°; Baroni et al., 2004). Abrupt transition to surrounding slopes and to the upper surfaces; light coloured with little surface weathering compared to surrounding stable slopes (Wahrhaftig and Cox, 1959; Janke and Bolch, 2021).	Gentle frontal slopes ($< 30^\circ$) and gentle transition to surrounding slopes and upper surface (Janke and Bolch, 2021).

activity as intact rock glaciers and relict rock glaciers. Intact landforms are further subdivided into: (i) active landforms, which contain ice and display movement and (ii) inactive landforms, which contain ice and no longer display movement. Relict rock glaciers are those which do not contain ice nor display movement (Haeberli, 1985; Barsch, 1996). This nomenclature follows our previous work (e.g. Jones et al., 2018a, 2018b, 2021). Rock glaciers differ from debris-covered glaciers, which are characterized by fully or partially covered tongues of up to tens of kilometers in length, with supraglacial features such as ice cliffs, supraglacial lakes, debris cones/hummocks and depressions (Racoviteanu et al., 2022b).

The methodology of identification and digitisation of rock glaciers was described in detail in Jones et al. (2018b) for the Nepal Himalaya. To expand the area estimates to the entire Himalaya, we followed the same methodology: a uniform grid of $\sim 25 \text{ km}^2$ grid squares was created in ArcGIS in vector format and then imported to Google Earth Pro and overlaid on the background satellite imagery. We systematically searched each grid square to identify both intact and relict rock glaciers. Each time a landform was found, its position was labelled using a digital “pin” (a vector marker) in Google Earth Pro. To ensure consistency, each pin point was digitized at the elevation at which the base of the frontal slope met the slope downstream so that the mean elevation at the front (MEF) of each feature could be extracted. A $\sim 5\%$ sample of the identified landforms was randomly selected from the Western, Central and Eastern Himalaya respectively within ArcGIS using the Subset Features tool. The small sample size was chosen for pragmatic reasons, i.e., because of the large size of the spatial domain. The resulting sample comprised of landforms in the Western Himalaya [$n = 363$], central Himalaya [$n = 192$] and Eastern Himalaya [$n = 378$], with a total of 933 intact and relict rock glacier samples. In order to estimate the total landform area, the point database presented here [$n = 933$] was amalgamated with the existing systematic rock glacier inventory for the Nepalese Himalaya (Jones et al., 2018b) [$n = 1137$], resulting in a sample of 2070 rock glaciers (Fig. 1). These were manually digitized on the Google Earth imagery using the geomorphic criteria as described in Jones et al. (2018b). From this sample, we assessed the quantitative and qualitative characteristics of rock glaciers then aggregated these across the three Himalaya regions.

3.3. Rock glacier upscaling

Our rock glacier sample was then extended to the entire population on a regional basis through the following upscaling procedure:

- Calculated the mean area [$\bar{A}_{\text{subsampled}}$] and total area [$A_{\text{subsampled}}$] of the subsampled rock glaciers [$N_{\text{subsampled}}$]

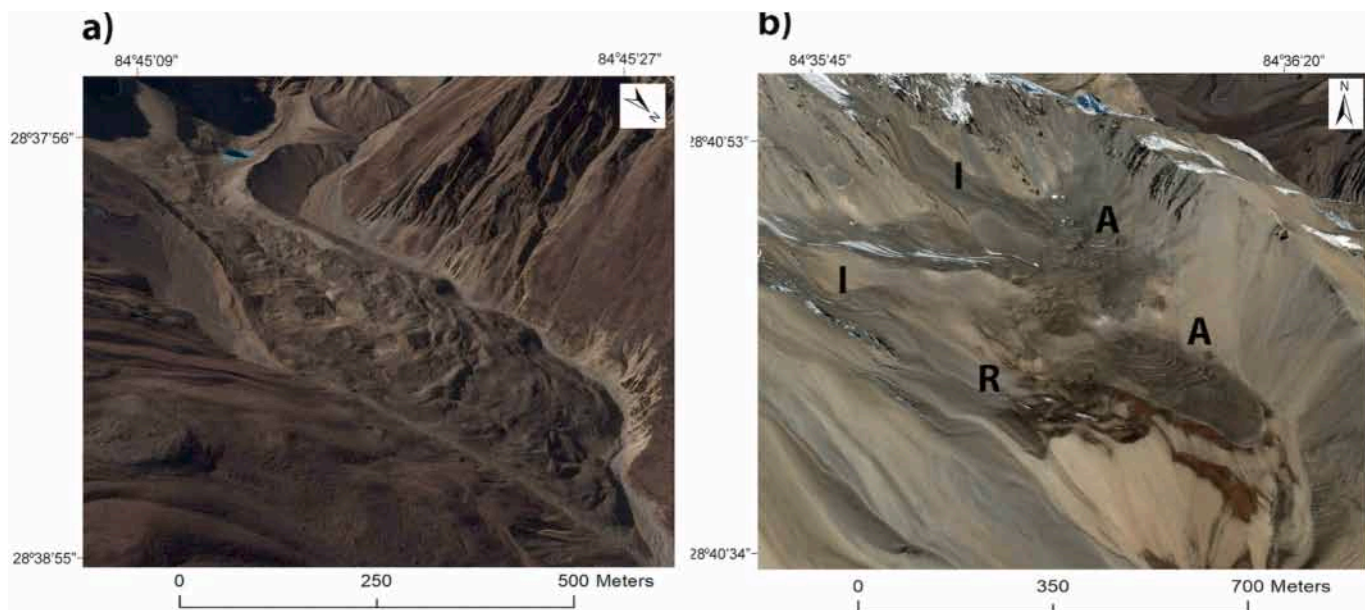


Fig. 2. Examples of intact and relict rock glaciers in the Manaslu region of Nepal. (a) active rock glacier and (b) rock glacier complex with active ('A'), inactive ('I') (and relict ('R') rock glaciers.

- Determined the number of remaining unsampled rock glaciers: $[N_{\text{unsampled}} = N_{\text{pinned}} - N_{\text{subsampled}}]$
- Calculated the additional area of the unsampled glaciers using the mean area from the sampled ones: $[A_{\text{unsampled}} = \bar{A}_{\text{subsampled}} * N_{\text{unsampled}}]$
- Calculated the total upscaled area: $A_{\text{tot}} = A_{\text{unsampled}} + A_{\text{subsampled}}$

3.4. Validation analysis

To assess the uncertainty of the upscaling method, we used the Manaslu region of Nepal (Fig. 1) as a test area. Rock glacier outlines were digitized on a false colour composite of the 2019 RapidEye image (bands 4, 3, 2) and the high-resolution basemaps from ESRI, using the geomorphic criteria listed in the revised IPA guidelines (RGIK, 2022). Following these guidelines, we mapped the rock glacier polygons based on the following geomorphic criteria: (i) presence of a discernible talus slope at the front usually displaying a convex morphology perpendicular to the principal (former) flow direction; (ii) presence of lateral margins as a discernible continuation of the front and (iii) presence of the characteristics ridge-and-furrow topography, identified as pronounced convex-downslope or longitudinal-surface undulations associated with current or former compressive flow (RGIK, 2022). Where visible, we digitized the rooting area of each rock glacier. Rock glaciers were digitized for each location of a “pin” identified in Jones et al. (2018a, 2018b). We used the extended geomorphological footprint, i. e. the rock glacier outline embeds the entire rock glacier up to the rooting zone, including the external parts (front and lateral margins) (RGIK, 2022). The digitized rock glacier polygons were taken to represent “ground truth”. For each glacier, we calculated the min, mean and maximum digitized area, and the elevation range extracted on the basis of the AW3D30 DEM (JAXA, 2019). The resulting total digitized area was compared to the total upscaled area for the Manaslu region to estimate the uncertainty of the proposed upscaling technique at a regional level. For the purposes of the area comparison only, we did not evaluate the area differences separately for each of the two subclasses of rock glaciers (intact or relict). We also present the distribution of rock glaciers with respect to clean and debris-covered glaciers in the Manaslu region based on datasets from a previous study (Racoviteanu et al., 2022a).

4. Results and discussion

4.1. Rock glacier distribution and area estimates across the Himalaya

A total of 24,968 landforms were identified across the Himalaya and “pinned” in Google Earth; this consists of both intact rock glaciers and relict rock glaciers. This represents an additional 18,729 landforms compared to the previous inventory for Nepal Himalaya, reported in Jones et al., 2018b. The sampled landforms [$n = 2070$] across the Himalaya cover a total surface area of 359.95 km² with intact rock glaciers [$n = 1371$] covering 277.78 km² (~ 77% of the total coverage) and relict rock glaciers [$n = 699$] covering 82.18 km² (~ 23% of the total coverage). The total sampled landform surface coverage is largest in the Central Himalaya (278.70 km²), succeeded by the Western Himalaya (53.76 km²) and Eastern Himalaya (27.50 km²). Here, when reporting sample totals, it is important to note the proportionally larger sample size for the Central Himalaya, which is the result of the amalgamation of the database presented here with the existing systematic rock glacier inventory for the Nepalese Himalaya (Jones et al., 2018b). Correspondingly, the mean surface area of all sampled landforms (intact and relict) is greatest in the Central Himalaya (0.21 km²) followed by the Western Himalaya (0.15 km²), with the smallest landforms in the Eastern Himalaya (0.07 km²) (see Table 2). In general, for all three regions, relict rock glaciers are on average smaller than intact rock glaciers (14–33% area difference), with the largest difference in the Central Himalaya (Table 2).

Inactive and relict rock glaciers accounted for ~65% ($n = 16,334$) and ~35% ($n = 8634$) of the total identified landforms in the Himalaya, respectively, based on upscaled estimates (Table 2). Approximately 40% ($n = 10,060$) of these landforms are located in the Central Himalaya, ~30% ($n = 7573$) in the Eastern Himalaya and ~29% ($n = 7335$) in the Western Himalaya (Table 2). Across the Himalaya, intact rock glacier mean density is 0.05 and relict rock glacier mean density is 0.02 (Jones et al., 2019 unpublished data). Direct conversion of specific relict rock glacier/intact rock glacier area (ha km⁻²) to specific relict rock glacier/intact rock glacier density (%) enables comparison with previous studies. At 1.05%, the specific landform density we estimate for the entire Himalaya is lower than for other regional studies across HMA. For example, Bolch and Gorbunov (2014) record this as ~1.50% in the Northern Tien Shan (Kazakhstan/Kyrgyzstan); 2.65% in the Zailiyskiy

Table 2

Key mean characteristics for intact rock glaciers (IRG) and relict rock glaciers (RRG) for the subsample of rock glaciers [n = 2070] and the number of upscaled glaciers in each region.

Region	Type	No.	%	MEF (masl)	Max E (masl)	Length (m)	Width (m)	Area (km ²)	Aspect	No. of landforms (upscaled)
Eastern	IRG	199	53	5036	5158	413	172	0.08	NW	3987
	RRG	179	47	4852	4956	343	145	0.06	NW	3586
	All	378	–	4949	5062	380	159	0.07	NW	7573
Central	IRG	897	67	4989	5220	748	261	0.24	NW	6790
	RRG	432	33	4599	4785	518	219	0.14	NW	3270
	All	1329	–	4863	5078	673	248	0.21	NW	10,060
Western	IRG	275	76	4564	4729	587	223	0.15	NW	5557
	RRG	88	24	4312	4470	546	188	0.13	N	1778
	All	363	–	4503	4666	577	215	0.15	NW	7335
Total	IRG	1371	66	4911	5112	667	241	0.20	NW	16,334
	RRG	699	34	4628	4789	477	196	0.12	NW	8634
	All	2070	–	4815	5003	603	226	0.17	NW	24,968

and Kungey Alatau (Kazakhstan/Kyrgyzstan) (Bolch and Marchenko, 2006) and 3.40% in the Nepalese Himalaya (Jones et al., 2018b). However, as the Tibetan Plateau constitutes a significant proportion of the terrain ≥ 3225 m a.s.l., this may suppress the specific landform density values presented here.

Across the entire region, the area of individual sampled landforms varies between 0.004 km^2 and 3.54 km^2 , with 1069 landforms $\geq 0.1\text{ km}^2$ in area. Considered individually, the largest sampled intact rock glacier (3.54 km^2) and relict rock glacier (1.50 km^2) are both located in the Central Himalaya. In the Himalaya, the estimated total upscaled relict rock glacier and intact rock glacier area is 3747 km^2 , representing $\sim 16\%$ of the area covered by glaciers in the same region ($22,829\text{ km}^2$). At the mountain-range scale, relict rock glacier and intact rock glacier coverage ranged between 550.87 km^2 and 2109.63 km^2 in the East and Central Himalaya, respectively (see Jones et al., 2021 for details).

We found that in the Himalaya, several relict rock glaciers and intact rock glaciers have similar areal coverage to the largest examples found elsewhere. Onaca et al. (2017) speculate that rock glaciers in the highest elevation mountain ranges are comparatively larger than those situated in lower mountain ranges, and they link this to the longevity of activity. Additionally, given the importance of debris-supply to rock glacier development and persistence, Hewitt (2014, p. 276) notes that the size and frequency of rock glaciers increases with height of the interfluvia (see also Olyphant, 1983; Haeberli et al., 2006). In the high and deeply incised ranges of the Himalaya (Scherler et al., 2011), it is reasonable to assume that these topographic factors have considerable influence on relict rock glacier/intact rock glacier size, although this hypothesis has not been tested here.

4.2. Elevation and topographic characteristics

Across the Himalaya, the sampled relict rock glaciers and intact rock glaciers [n = 2070] have a minimum elevation at the front (MEF) ranging from 3225 to 5766 m a.s.l., with the lowest found for a rock glacier located in the Central Himalaya. The mean density ($n\text{ km}^{-2}$) of sampled intact and relict rock glaciers at elevations ≥ 3225 m a.s.l. ranges from 0.06 (West Himalaya) to 0.08 (Eastern /Central Himalaya) (Table 3). A total of 87% of the sampled landforms were found between 4200 and 5400 m a.s.l. This is broadly consistent with that previously reported for the Hindu Kush region (3554–5735 m a.s.l.) (Schmid et al., 2015). At the regional-scale, mean MEFs for the Eastern (4949 ± 256 m a.s.l.), Central (4863 ± 372 m a.s.l.) and Western Himalaya (4503 ± 422 m a.s.l.) show a decreasing westward trend in inactive and relict rock glacier elevation across the Himalaya (Fig. 3). This trend remains consistent when considering relict rock glaciers and intact rock glaciers separately. Furthermore, in agreement with Schmid et al. (2015), we report a pronounced south-to-north increase in inactive and relict rock glacier MEF across the Himalaya, with relict rock glaciers/rock glaciers found typically, several hundreds of metres higher on the northern

Table 3

Intact Rock glacier (IRG)/Relict rock glacier (RRG) proportion, proportional area ≥ 3225 m a.s.l., density in specific regions of the Himalaya. Where appropriate, values are reported to two decimal places. *Density ($n\text{ km}^{-2}$) was calculated considering the area ≥ 3225 m a.s.l. (MEF of lowest observed landform). † Specific area (hakm^{-2}) where ha reflects intact rock glacier/relict rock glacier area was calculated considering the regional area ≥ 3225 m asl. The upscaled results were used in calculations of both density and specific area.

	Eastern Himalaya	Central Himalaya	Western Himalaya
IRG/RRG proportion	30%	30%	40%
Proportional area ≥ 3225 m a.s.l.	26%	37%	37%
Density ($n\text{ km}^{-2}$)*	0.08	0.08	0.06
Specific area (hakm^{-2})†	0.59	1.60	0.82

slopes (Table 4 and Fig. 4). As expected, across the Himalaya, inactive rock glaciers are located at higher elevations than relict rock glaciers and this pattern is statistically significant based on the ANOVA test ($p \leq 0.001$, 99% confidence level). Tukey post hoc test results show that this finding also exists at the regional-scale (Western Himalaya: Diff = 252 m, $p \leq 0.001$; Central Himalaya: Diff: 390 m, $p \leq 0.001$; Eastern Himalaya: Diff = 184 m, $p \leq 0.001$). Across the entire Himalaya, intact rock glaciers are predominantly found above 4800 m a.s.l. (65%) with relict rock glaciers found below 4800 m a.s.l. (67%). Furthermore, rock glaciers are clustered between 4400 and 5400 m a.s.l. (84%) and relict rock glaciers between 4200 and 5200 m a.s.l. (79%). This result provides validation for the dynamic status classification, given the expected vertical progression of suitable habitats for rock glacier development and persistence linked to climate warming.

With respect to slope aspect, across the Himalaya, sampled relict rock glaciers/intact rock glaciers are primarily situated on northern quadrants (NW: 17%; NE: 16%; N: 16%; 3, Table 4 and Fig. 4). Furthermore, the mean aspect of relict rock glaciers/intact rock glaciers shows that they cluster around north-western slopes (*mean orientation* = 321°). Regionally, a greater proportion of intact rock glaciers (40–57%) are situated within the northern quadrant compared to the southern quadrant (20–32% intact rock glaciers). Similarly, relict rock glaciers are also predominantly located within the northern quadrant (57–62%) compared to the southern quadrant (13–19%). Circular variance indicates that relict rock glaciers have lower dispersal (0.39) than intact rock glaciers (0.20), with proportionally more relict features located on northerly slopes compared to intact rock glaciers. In addition, across the Himalaya these landforms situated within the northern aspect quadrant occur at lower elevations than those found within the southern aspect quadrant (Fig. 4) also illustrates the clustering of relict rock glaciers and intact rock glaciers around northerly aspects. The results presented here corroborate the findings of other northern hemispheric studies, which

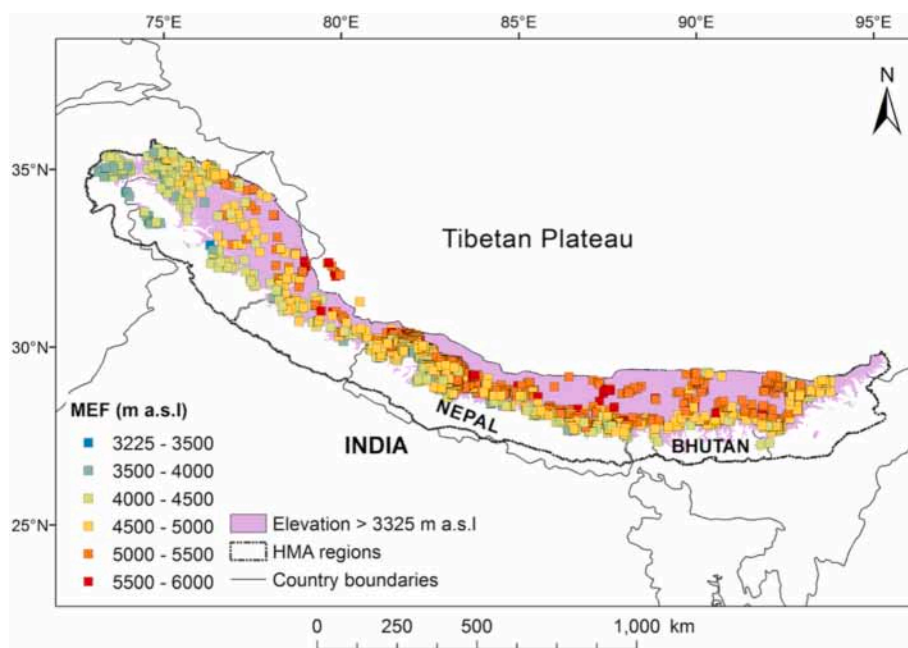


Fig. 3. Mean Elevation at the Front (MEF) for the sampled intact and relict rock glaciers across the Himalaya. The area showed in purple over the entire range represents the terrain above the minimum elevation (3225 m a.s.l.) at which rock glaciers were found. (For interpretation of the references to colour in this figure legend, the reader is referred to the web version of this article.)

Table 4

Regional aspect classification of rock glaciers (RG) and relict rock glaciers (RRG) into north- (292.5 to 67.5°) and south- (112.5 to 247.5°) facing aspect quadrants.

Activity	Aspect Quadrant	Eastern Himalaya	Central Himalaya	Western Himalaya
IRG	North (NW, N, NE)	46%	40%	57%
	South (SW, S, SE)	24%	32%	20%
RRG	North (NW, N, NE)	62%	58%	57%
	South (SW, S, SE)	13%	19%	18%

have detailed similar microclimatic relationships (e.g., Ishikawa et al., 2001; Seppi et al., 2012; Scotti et al., 2013; Baral et al., 2019). Therefore, it is reasonable to assume that northerly aspects with their reduced solar insolation, enable rock glacier formation and preservation at lower elevations than other aspects. These slopes may also be steeper than those of other aspects having undergone likely longer periods of glacial erosion during Quaternary times, and therefore are more able to produce elevated debris fluxes to valley floors.

4.3. Validation in the Manaslu region of Nepal

In the Manaslu region, manual mapping of intact and relict rock glaciers based on high-resolution imagery yielded a total of 487 polygons with an area of 68.5 km², ranging from 0.006 to 1.33 km², with a mean area of 0.18 km² and elevations ranging from 3839 m to 6127 m a.s.l. (Table 5). Over the same area, a total of 452 rock glaciers had been “pinned” in Jones et al. (2018b) as described earlier; of these, 59 intact and relict rock glaciers had been sampled, ranging in area from 0.01 to 1.38 km², with a total area of 11.12 km² and a mean area of 0.18 km² (Table 5). Based on the mean area from the sample of 59 intact and relict rock glaciers, the area for the remaining 393 unsampled rock glaciers was calculated as 70.74 km² using the method described earlier (Section 3.3). On this basis, the total upscaled area of intact and relict rock

glaciers in this region (sampled and unsampled) was 81.86 km².

Compared to the area of the landforms manually digitized previously from Google Earth (68.5 km²), this yields an overestimation of 13.4 km² (~16%) based on the upscaled area (Fig. 5). We note that while intact and relict rock glaciers tend to be smaller in size compared to both clean and debris-covered glaciers, they are abundant in the Manaslu region and cover relatively similar area to the debris-covered ice (68.5 km² vs. 71.6 km²). However, there remain large uncertainties in the area delineation of rock glaciers, notably the omission in some cases of the rooting zone which is less visible than the rest of the glacier.

4.4. Considerations on uncertainty

Uncertainty sources in this study comprise (a) the uncertainty in determining the presence of rock glacier on Google Earth imagery, (b) mapping of the rock glacier boundaries and (c) the classification of rock glaciers as intact or relict. Uncertainty related to (a) is subject to analyst expertise and the quality of the imagery available in Google Earth. For example, some areas may be cloud covered at the time of image acquisition thus making the identification of rock glaciers difficult or impossible. With respect to (b), the upscaled area approach is sensitive to the mean area of rock glaciers chosen on a sub-region basis, which is in turn influenced by the quality of the mapped rock glaciers. Manually digitized boundaries, however, are also subject to a variety of errors, notably due to misinterpretation of the upper part (rooting zone) of rock glaciers, which can lead to uncertainties in rock glacier area and number of rock glaciers identified (by a factor of three in both cases) (Brardinoni et al., 2019; Cai et al., 2021). Orthoimages from base maps may also be distorted, further creating errors in the rock glacier surface (Marcer et al., 2019); however, we estimate these to be minimal because multiple orthoimages from various sources were used. Errors in the digitization of the rooting zone affect the calculation of the maximum altitude but less so the MEF of the rock glacier sample. With respect to the classification of rock glaciers (c), this was performed qualitatively by the analyst based on morphological characteristics (Borsch, 1996). While this is the common approach adopted as in most studies (Onaca et al., 2017; Brardinoni et al., 2019), this remains subjective and dependent on analyst experience. To mitigate all these sources of errors, multiple

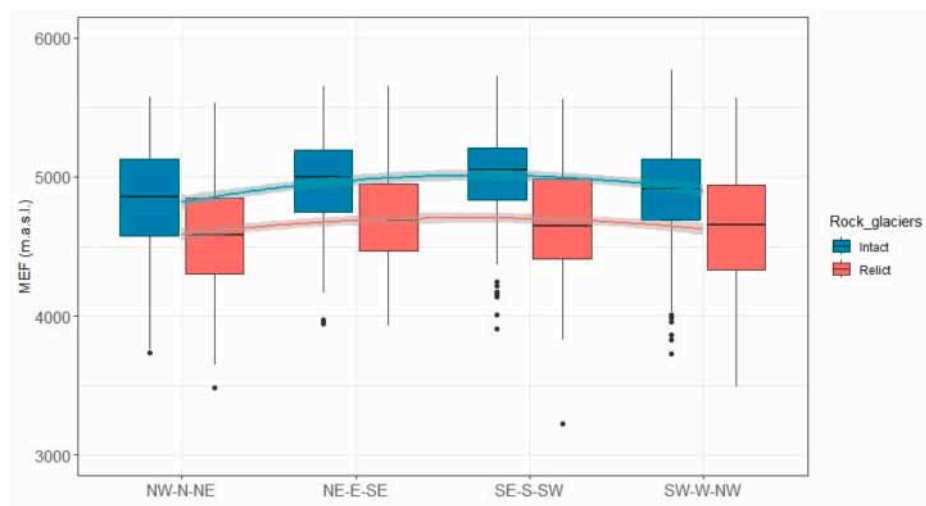


Fig. 4. Boxplots showing the distribution of intact (I-DLs) and relict rock glaciers (DDAs) across the Himalaya by aspect and elevation. The smooth lines display the polynomial regression models of mean MEF (m.a.s.l.) with aspect group for intact and relict glaciers. The polynomial regression model for the mean MEF and aspect of intact rock glaciers is:

$$y_1 = -65.506x_1^2 + 354.98x_1 + 4529.3 \quad (1)$$

and the polynomial regression model for the mean MEF and aspect of relict rock glaciers is:

$$y_2 = -43.385x_2^2 + 229.96x_2 + 4400 \quad (2)$$

where x represents the aspect group, and y represents mean MEF.

The distance between peak MEF of intact and relict rock glaciers can be calculated through (1) and (2). When $x_1 = 2.71$, y_1 is the peak value of 5010; when $x_2 = 2.65$, y_2 is the peak value of 4705. The MEF difference between intact and relict rock glaciers is therefore 305 m.a.s.l.

Table 5

Distribution and basic statistics of clean, debris-covered and rock glaciers in the Manaslu region of the Himalaya.

Glacier type	no. glaciers	Area (km ²)				Elevation		
		min	max	mean	total	min	max	mean
Clean ice	455	0.004	34.5	1.4	639.9	3270	7959	5739
Debris-covered ice	45	0.030	11.1	1.6	71.6	3273	5834	4719
Rock glaciers	487	0.006	1.3	0.18	68.5	3839	6127	5017

analysts can be used in a future study; however, at Himalaya scale this remains time consuming.

Accurate remote mapping of rock glaciers is furthermore hampered by the uncertainties associated with mimicry (e.g. Whalley and Martin, 1992; Harrison et al., 2008; Jarman et al., 2013). This is most clearly seen in the ways in which rock slope failures often mimic some of the characteristics of rock glaciers. Jarman et al. (2013) and Jarman and Harrison (2019) identify the following four issues. First, transverse ridges are characteristic of rock glaciers, but also often develop in RSF where the rapidly moving mass decelerates quickly, producing compression ridges, and subsides, producing extension ridges. Second, randomly distributed hollows exist in rock glaciers and reflect the melting of ice cores; they also occur when coarse disintegrated rock masses come to rest after rapid downslope movement. Third, arcuate lobes, tongues and perimeter ridges are characteristic of rock glaciers but also occur on RSF where rockslides emanate from confined sources and debouch onto open footslopes. Finally, intact rock glaciers display steep frontal margins; these also occur on rock slope failures where the sliding mass rapidly loses momentum as gradients flatten.

While the distribution of rock slope failures in the Himalaya is not currently known, they must be common given the combination of steep and extensive rock slopes, rapid warming of permafrost and high frequency of seismic activity. As a result, the opportunity for

misidentification of rock slope failures as rock glaciers (and vice versa) is likely to be high.

4.5. Future work and conclusions

We have previously suggested that rock glaciers in HMA might become more numerous in future, and of increased importance in providing water supplies as ice glaciers undergo continued recession (Jones et al., 2019; Jones et al., 2021; Harrison et al., 2021). Climate model simulations project sustained reduction in glacier mass balance over the coming century in most areas of the Himalaya and wider HMA (e.g. Shannon et al., 2019; Jones et al., 2021) and we have argued previously (e.g. Harrison et al., 2021) that intact rock glaciers might therefore become more important for maintaining water supplies as ice glaciers melt. While the impact of rock glaciers on surface runoff at the catchment scale might be negligible, we argue that their role in providing water for groundwater might be significant (Brighenti et al., 2019; Wagner et al., 2020; 2021). We have also hypothesised that existing debris-covered glaciers and debris-covered glacier tongues might undergo a transition to rock glaciers (Jones et al., 2019; Knight et al., 2019). Important questions follow from this, including: how might this transition occur, which glaciers might undergo this transition, how quickly might this transition occur, and what are the water supply

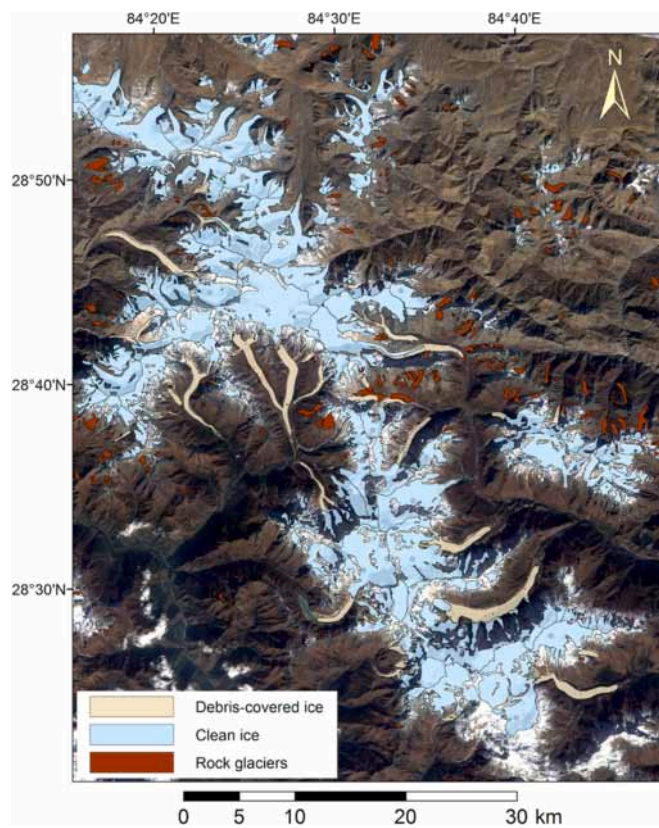


Fig. 5. Distribution of clean, debris-covered and rock glaciers in the Manaslu region of Nepal. Clean and debris-covered extents were delineated in a previous study (Racoviteanu et al., 2022a); rock glacier extents were manually digitized in this study based on RGIK (2022) guidelines as described in Section 3.4. Background imagery is a true colour composite (bands 4, 3, 2) of RapidEye imagery from November 2019.

implications that follow. The answers to these are, at present, unknown but we can hypothesise that this transition will have profound impacts on future water supplies (Jones et al., 2021; Harrison et al., 2021).

We have presented the first systematic estimate of intact and relict rock glacier coverage for the Himalaya and shown that there are approximately 25,000 such features with an area coverage of ~ 3747 km 2 . This is the most extensive systematic inventory (in terms of total rock glaciers and relict rock glaciers number and areal coverage), conducted globally to date. The landforms identified and analysed regionally across three regions of the Himalaya (Western Himalaya, Central Himalaya and Eastern Himalaya) showed that the majority of these landforms ($\sim 65\%$) were intact rock glaciers (i.e. I-DL) and the remainder were relict rock glaciers (i.e. DDAs). Rock glaciers in the Himalaya constitute hydrologically valuable long-term water stores and given continued climatically-driven glacier recession and mass loss the relative hydrological value of rock glaciers in mountain regions will likely become increasingly important. Prior to this study, knowledge of Himalaya-wide rock glaciers and relict rock glaciers characteristics was largely missing, and so our work provides the first scientific baseline from which Himalayan-wide rock glacier and wider cryosphere response to climate change can be assessed.

CRediT authorship contribution statement

Stephan Harrison: Supervision, Methodology, Investigation, Funding acquisition, Conceptualization, Writing – review & editing, Writing – original draft. **Darren B. Jones:** Investigation, Formal analysis, Data curation, Conceptualization, Writing – original draft. **Adina E. Racoviteanu:** Visualization, Validation, Methodology, Formal analysis, Data

curation, Writing – review & editing. **Karen Anderson:** Supervision, Writing – review & editing. **Sarah Shannon:** Visualization, Software, Investigation, Formal analysis. **Richard A. Betts:** Formal analysis. **Ruolin Leng:** Formal analysis.

Declaration of competing interest

The authors declare that they have no known competing financial interests or personal relationships that could have appeared to influence the work reported in this paper.

The authors declare the following financial interests/personal relationships which may be considered as potential competing interests:

Darren Jones reports financial support was provided by Natural Environment Research Council. Stephan Harrison, Darren Jones reports financial support was provided by Royal Geographical Society. Richard Betts reports was provided by Department for Business, Energy and Industrial Strategy. If there are other authors, they declare that they have no known competing financial interests or personal relationships that could have appeared to influence the work reported in this paper.

Data availability

Data are available at the zenodo link(10.5281/zenodo.11237094)

Acknowledgements

DBJ was supported by a research grant from the Natural Environment Research Council (Grant No. NE/L002434/1) and the Royal Geographical Society (with IBG) through a Dudley Stamp Memorial Award. SH was in receipt of a Walters-Kundert RGS Fellowship for fieldwork in the Himalaya, and RAB was supported by the Met Office Hadley Centre Climate Programme funded by BEIS. A. Racoviteanu's work was supported by the ENSURE programme grant 2021 and the French National Research Institute for Sustainable Development (IRD). We thank the reviewers and the editor whose comments significantly improved the paper.

References

- Baral, P., Haq, M.A., Yaragal, S., 2019. Assessment of rock glaciers and permafrost distribution in Uttarakhand, India. *Permafro. Periglac. Process.* 31 <https://doi.org/10.1002/ppp.2008>.
- Baroni, C., Carton, A., Seppi, R., 2004. Distribution and behaviour of rock glaciers in the Adamello-Presanella Massif (Italian Alps). *Permafro. Periglac. Process.* 15 (3), 243–259.
- Barros, A.P., Lang, T.J., 2003. Monitoring the Monsoon in the Himalayas: Observations in Central Nepal, June 2001. *Mon. Weather Rev.* 1408–1427.
- Barsch, D., 1996. Rockglaciers: Indicators for the Present and Former Geocology in High Mountain Environments. Berlin, Germany, Springer-Verlag, Berlin Heidelberg. p. 1.
- Berthling, I., 2011. Beyond confusion: Rock glaciers as cryo-conditioned landforms. *Geomorphology* 131 (3–4), 98–106. <https://doi.org/10.1016/j.geomorph.2011.05.002>.
- Blöthe, J.H., Rosenwinkel, S., Höser, T., Korup, O., 2019. Rock-glacier dams in High Asia. *Earth Surf. Process. Landf.* 44, 808–824. <https://doi.org/10.1002/esp.4532>.
- Bolch, T., Gorbunov, A.P., 2014. Characteristics and origin of rock glaciers in Northern Tien Shan (Kazakhstan/Kyrgyzstan). *Permafro. Periglac. Process.* 25 (4), 320–332. <https://doi.org/10.1002/ppp.1825>.
- Bolch, T., Marchenko, S.S., 2006. Significance of Glaciers, Rockglaciers and Ice-Rich Permafrost in the Northern Tien Shan as Water Towers under Climate Change Conditions. Proceedings of the Workshop Assessment of Snow-Glacier and Water Resources in Asia, Almaty, Kazakhstan, IHP/HWRP-Berichte.
- Bolch, T., Kulkarni, A., Kääb, A., Huggel, C., Paul, F., Cogley, J.G., Frey, H., Kargel, J.S., Fujita, K., Scheel, M., Bajracharya, S., Stoffel, M., 2012. The State and Fate of Himalayan Glaciers. *Science* 336 (6079), 310.
- Bolch, T., Shea, J.M., Liu, S., Azam, F.M., Gao, Y., Gruber, S., Immerzeel, W.W., Kulkarni, A., Li, H., Tahir, A.A., Zhang, G., Zhang, Y., 2019. Status and Change of the Cryosphere in the Extended Hindu Kush Himalaya Region. In: Wester, P., Mishra, A., Mukherji, A., Shrestha, A.B. (Eds.), *The Hindu Kush Himalaya Assessment: Mountains, Climate Change, Sustainability and People*. Springer International Publishing, Cham, pp. 209–255. https://doi.org/10.1007/978-3-319-92288-1_7.
- Bookhagen, B., Burbank, D.W., 2006. Topography, relief and TRMM-derived rainfall variations along the Himalaya. *Geophys. Res. Lett.* 33. <https://doi.org/10.1029/2006gl026037>.

Brardinoni, F., Scotti, R., Sailer, R., Mair, V., 2019. Evaluating sources of uncertainty and variability in rock glacier inventories. *Earth Surf. Process. Landf.* 44 <https://doi.org/10.1002/esp.4674>.

Brightoni, S., Tolotti, M., Bruno, M.C., Engel, M., Wharton, G., Cerasino, L., Mair, V., Bertoldi, W., 2019. After the peak water: the increasing influence of rock glaciers on alpine river systems. *Hydrol. Process.* 33 (21), 2804–2823.

Buckel, J., Reinosch, E., Voigtlander, A., Dietze, M., Bücker, M., Krebs, N., Schroeckh, R., Mäusbacher, R., Hördt, A., 2022. Rock glacier characteristics under semiarid climate conditions in the Western Nyainqntanglha range, Tibetan Plateau. *J. Geophys. Res. Earth Surf.* e2021JF006256.

Cai, J., Wang, X., Liu, G., Yu, B., 2021. A Comparative Study of active Rock Glaciers Mapped from Geomorphic- and Kinematic-based Approaches in Daxue Shan, Southeast Tibetan Plateau. *Remote Sens.* 13 (23) <https://doi.org/10.3390/rs13234931>.

Caretta, M.A., et al., 2022. Chapter 4: Water. in: Climate Change 2022: Impacts, Adaptation and Vulnerability. In: Pörtner, H.-O., et al. (Eds.), Working Group II contribution to the Sixth Assessment Report of the Intergovernmental Panel on Climate Change. Cambridge University Press, pp. 1–148.

Chakravarti, P., Jain, V., Mishra, V., 2022. The distribution and hydrological significance of intact rock glaciers in the north-west Himalaya. *Geogr. Ann. Ser. A Phys. Geogr.* 104 (3), 226–244.

Delaloye, R., Perruchoud, E., Avian, M., Kaufmann, V., Bodin, X., Hausmann, H., Ikeda, A., Kääb, A., Kellerer-Pirkbauer, A., Krainer, K., 2008. Recent Interannual Variations of Rock Glacier Creep in the European Alps.

Erhardt, G.H., Wagner, T., Winkler, G., Marcher, T., 2022. Machine learning – an approach for consistent rock glacier mapping and inventorying – example of Austria. *Appl. Comput. Geosci.* 16, 100093 <https://doi.org/10.1016/j.acags.2022.100093>.

Falaschi, D., Castro, M., Masiocci, M., Tadono, T., Ahumada, A., 2014. Rock glacier inventory of the Valles Calchaquíes region (~ 25 S), Salta, Argentina, derived from ALOS data. *Permafrost. Periglac.* 25, 69–75.

Fountain, A.G., Walder, J.S., 1998. Water flow through temperate glaciers. *Rev. Geophys.* 36 (3), 299–328. <https://doi.org/10.1029/97RG03579>.

Fox-Kemper, B., Hewitt, H.T., Xiao, C., Aðalgeirsdóttir, G., Drijfhout, S.S., Edwards, T.L., Golledge, N.R., Hemer, M., Kopp, R.E., Krinner, G., Mix, A., 2021. 2021: Ocean, cryosphere and sea level change. *Climate Change 2021: The Physical Science Basis. Contribution of Working Group I to the Sixth Assessment Report of the Intergovernmental Panel on Climate Change*. Cambridge University Press.

Fyffe, C.L., Brock, B.W., Kirkbride, M.P., Mair, D.W.F., Arnold, N.S., Smiraglia, C., Diolaiuti, G., Diotri, F., 2019. Do debris-covered glaciers demonstrate distinctive hydrological behaviour compared to clean glaciers? *J. Hydrol.* 570, 584–597. <https://doi.org/10.1016/j.jhydrol.2018.12.069>.

Haeberli, W., 1985. Creep of mountain permafrost: internal structure and flow of alpine rock glaciers. *Mitteilungen der Versuchsanstalt für Wasserbau, Hydrologie und Glaziologie an der Eidgenössischen Technischen Hochschule Zürich*, (77).

Haeberli, W., Hallet, B., Areson, L., Elconin, R., Humlum, O., Kääb, A., Kaufmann, V., Ladanyi, B., Matsuoka, N., Springman, S., Mühl, D.V., 2006. Permafrost creep and rock glacier dynamics. *Permafrost. Periglac.* 17 (3), 189–214. <https://doi.org/10.1002/ppp.561>.

Harrison, S., Whalley, B., Anderson, E., 2008. Relict rock glaciers and protalus lobes in the British Isles: implications for late Pleistocene mountain geomorphology and palaeoclimate. *J. Quat. Sci.* 23 (3), 287–304.

Harrison, S., Jones, D., Anderson, K., Shannon, S., Betts, R.A., 2021. Is ice in the Himalayas more resilient to climate change than we thought? *Geogr. Ann. Ser. B* 103 (1), 1–7.

Hassan, J.C., Chen, Xiaoqing, Muhammad, Sher, Bazai, Nazir Ahmed, 2021. Rock glacier inventory, permafrost probability distribution modeling and associated hazards in the Hunza River Basin, Western Karakoram, Pakistan. *Sci. Total Environ.* 782, 146833 <https://doi.org/10.1016/j.scitotenv.2021.146833>.

Hewitt, K., 2014. Rock glaciers and related phenomena. In: Hewitt, K. (Ed.), *Glaciers of the Karakoram Himalaya: Glacial Environments, Processes, Hazards and Resources*. Dordrecht, Springer Netherlands, pp. 267–289. https://doi.org/10.1007/978-94-007-6311-1_11.

Hock, R., Bliss, A., Marzeion, B.E.N., Giesen, R.H., Hirabayashi, Y., Huss, M., Radić, V., Slanger, A.B.A., 2019. GlacierMIP – a model intercomparison of global-scale glacier mass-balance models and projections. *J. Glaciol.* 65 (251), 453–467. <https://doi.org/10.1017/jog.2019.22>.

Huss, M., Hock, R., 2018. Global-scale hydrological response to future glacier mass loss. *Nat. Clim. Chang.* 8 <https://doi.org/10.1038/s41558-017-0049-x>.

Immerzeel, W.W., van Beek, L.P.H., Konz, M., Shrestha, A.B., Bierkens, M.F.P., 2012. Hydrological response to climate change in a glacierized catchment in the Himalayas. *Clim. Chang.* 110 (3), 721–736. <https://doi.org/10.1007/s10584-011-0143-4>.

Immerzeel, W.W., Lutz, A.F., Andrade, M., Bahl, A., Biemans, H., et al., 2020. Importance and vulnerability of the world's water towers. *Nature* 577 (7790), 364–369. <https://doi.org/10.1038/s41586-019-1822-y>.

Irvine-Fynn, T.D.L., Hodson, A.J., Moorman, B.J., Vatne, G., Hubbard, A.L., 2011. Polythermal glacier hydrology: a review. *Rev. Geophys.* 49 (4) <https://doi.org/10.1029/2010RG000350>.

Ishikawa, M., Watanabe, T., Nakamura, N., 2001. Genetic differences of rock glaciers and the discontinuous mountain permafrost zone in Kanchanjunga Himal, Eastern Nepal. *Permafrost. Periglac.* 12 (3), 243–253. <https://doi.org/10.1002/ppp.394>.

Janke, J.R., Bolch, T., 2021. Rock glaciers. Reference module in Earth systems and Environmental Sciences.

Jansson, P., Hock, R., Schneider, T., 2003. The concept of glacier storage: a review. *J. Hydrol.* 282 (1–4), 116–129. [https://doi.org/10.1016/S0022-1694\(03\)00258-0](https://doi.org/10.1016/S0022-1694(03)00258-0).

Jarman, D., Harrison, S., 2019. Rock slope failure in the British mountains. *Geomorphology* 340, 202–223.

Jarman, D., Wilson, P., Harrison, S., 2013. Are there any relict rock glaciers in the British mountains? *J. Quat. Sci.* 28 (2), 131–143.

JAXA, 2019. ALOS Global Digital Surface Model “ALOS World 3D- 30m”: Pp.

Jones, D.B., Harrison, S., Anderson, K., Betts, R.A., 2018a. Mountain rock glaciers contain globally significant water stores. *Sci. Rep.* 8 (1), 2834. <https://doi.org/10.1038/s41598-018-21244-w>.

Jones, D.B., Harrison, S., Anderson, K., Selley, H.L., Wood, J.L., Betts, R.A., 2018b. The distribution and hydrological significance of rock glaciers in the Nepalese Himalaya. *Glob. Planet. Chang.* 160 (Supplement C), 123–142. <https://doi.org/10.1016/j.gloplacha.2017.11.005>.

Jones, D.B., Harrison, S., Anderson, K., Whalley, W.B., 2019. Rock glaciers and mountain hydrology: a review. *Earth Sci. Rev.* 193, 66–90. <https://doi.org/10.1016/j.earscirev.2019.04.001>.

Jones, D.B., Harrison, S., Anderson, K., Shannon, S., Betts, R.A., 2021. Rock glaciers represent hidden water stores in the Himalaya. *Sci. Total Environ.* 793, 145368.

Kääb, A., Weber, M., 2004. Development of transverse ridges on rock glaciers: field measurements and laboratory experiments. *Permafrost. Periglac.* 15 (4), 379–391.

Knight, J., Harrison, S., Jones, D.B., 2019. Rock glaciers and the geomorphological evolution of deglacierizing mountains. *Geomorphology* 324, 14–24.

Kraaijenbrink, P.D.A., Bierkens, M.F.P., Lutz, A.F., Immerzeel, W.W., 2017. Impact of a global temperature rise of 1.5 degrees Celsius on Asia's glaciers. *Nature* 549, 257–260. <https://doi.org/10.1038/nature23878> <https://www.nature.com/articles/nature23878#supplementary-information>.

Lutz, A.F., Immerzeel, W.W., Shrestha, A.B., Bierkens, M.F.P., 2014. Consistent increase in High Asia's runoff due to increasing glacier melt and precipitation. *Nat. Clim. Chang.* 4 (7), 587–592. <https://doi.org/10.1038/nclimate2237> <http://www.nature.com/nclimate/journal/v4/n7/abs/nclimate2237.html#supplementary-information>.

Marcer, M., Bodin, X., Brenning, A., Schoeneich, P., Charvet, R., Gottardi, F., 2017. Permafrost favorability index: spatial modeling in the French Alps using a Rock Glacier Inventory. *Front. Earth Sci.* 5, 105.

Marcer, M., Serrano, C., Brenning, A., Bodin, X., Goetz, J., Schoeneich, P., 2019. Evaluating the destabilization susceptibility of active rock glaciers in the French Alps. *Cryosphere* 13 (1), 141–155. <https://doi.org/10.5194/tc-13-141-2019>.

Marcer, M., Bodin, X., Ciccoira, A., Cusicanqui, D., Echelard, T., Schoeneich, P., 2021a. Rock glaciers in the French Alps - inventory of displacement rates and orthoimages of destabilized landforms in the period 1945–2018. *PANGAEA*.

Marcer, M., Ciccoira, A., Cusicanqui, D., Bodin, X., Echelard, T., Obregon, R., Schoeneich, P., 2021b. Rock glaciers throughout the French Alps accelerated and destabilised since 1990 as air temperatures increased. *Commun. Earth Environ.* 2 (1), 81. <https://doi.org/10.1038/s43247-021-00150-6>.

Martin, H.E., Whalley, W.B., 1987. Rock glaciers. Part 1: Rock glacier morphology: Classification and distribution. *Prog. Phys. Geogr.* 11 (2), 260–282. <https://doi.org/10.1177/030913338701100205>.

Maurer, J.M., Schaefer, J.M., Rupper, S., Corley, A., 2019. Acceleration of ice loss across the Himalayas over the past 40 years. *Science. Advances* 5 (6). <https://doi.org/10.1126/sciadv.aav7266>.

Miles, K.E., Hubbard, B., Irvine-Fynn, T.D.L., Miles, E.S., Quincey, D.J., Rowan, A.V., 2020. Hydrology of debris-covered glaciers in High Mountain Asia. *Earth Sci. Rev.* 207, 103212 <https://doi.org/10.1016/j.earscirev.2020.103212>.

Miles, E., McCarthy, M., Dehecq, A., Kneib, M., Fugger, S., Pellicciotti, F., 2021. Health and sustainability of glaciers in High Mountain Asia. *Nat. Commun.* 12 (1) <https://doi.org/10.1038/s41467-021-23073-4>.

NASA-JPL, 2013. NASA Shuttle Radar Topography Mission Global 1 Arc Second [Data Set]. N. E. L. P. DAAC.

Olyphant, G., 1983. Computer simulation of rock-glacier development under viscous and pseudoplastic flow. *Geol. Soc. Ann. Bull.* 94. [https://doi.org/10.1130/0016-7606\(1983\)1194<1499:CSORDU>1132.1130.CO;1132](https://doi.org/10.1130/0016-7606(1983)1194<1499:CSORDU>1132.1130.CO;1132).

Onaca, A., Ardelean, F., Urdea, P., Magori, B., 2017. Southern Carpathian rock glaciers: Inventory, distribution and environmental controlling factors. *Geomorphology* 293 (Part B), 391–404. <https://doi.org/10.1016/j.geomorph.2016.03.032>.

Planet_Labs, 2021. Planet Imagery Product Specifications.

Potter Jr., N., Steig, E.J., Clark, D.H., Speece, M.A., Clark, G.T., Updike, A.B., 1998. Galena Creek rock glacier revisited—New observations on an old controversy. *Geogr. Ann. Ser. B* 80 (3–4), 251–265.

Pritchard, H.D., 2019. Asia's shrinking glaciers protect large populations from drought stress. *Nature* 569 (7758), 649–654. <https://doi.org/10.1038/s41586-019-1240-1>.

Racoviteanu, A.E., Glasser, N.F., Robson, B.A., Harrison, S., Millan, R., Kayastha, R.B., Kayastha, R., 2022a. Surface evolution and associated morphological changes on glaciers in the Manaslu region of Nepal from satellite imagery and UAV data (1970–2019). *Front. Earth Sci.* <https://doi.org/10.3389/feart.2021.767317>.

Racoviteanu, A.E., Nicholson, L., Glasser, N.F., Miles, E., Harrison, S., Reynolds, J.M., 2022b. Debris-covered glacier systems and associated glacial lake outburst flood hazards: challenges and prospects. *J. Geol. Soc. Lond.* 179 (3) <https://doi.org/10.1144/jgs2021-084> [jgs2021-084](https://doi.org/10.1144/jgs2021-084).

Rangecroft, S., Harrison, S., Anderson, K., Magrath, J., Castel, A.P., Pacheco, P., 2014. A first rock glacier inventory for the Bolivian Andes. *Permafrost. Periglac.* 25 (4), 333–343.

Regmi, D., 2008. Rock Glacier Distribution and the Lower Limit of Discontinuous Mountain Permafrost in the Nepal Himalaya. *Proceedings of the Ninth International Conference on Permafrost, Fairbanks, Alaska*.

Reinosch, E., Gerke, M., Riedel, B., Schwalb, A., Ye, Q., Buckel, J., 2021. Rock glacier inventory of the western Nyainqntanglha Range, Tibetan Plateau, supported by

InSAR time series and automated classification. *Permafro. Periglac. Process.* 32 (4), 657–672. <https://doi.org/10.1002/ppp.2117>.

RGIK, 2022. Towards standard guidelines for inventorying rock glaciers: baseline concepts (version 4.2.2). *I. A. G. R. g. i. a. Kinematics* 13.

Robson, B.A., Nuth, C., Nielsen, P.R., Girod, L., Hendrickx, M., Dahl, S.O., 2018. Spatial Variability in patterns of Glacier Change across the Manaslu Range, Central Himalaya. *Front. Earth Sci.* 6, 12.

Robson, B.A., Bolch, T., MacDonell, S., Höhlbling, D., Rastner, P., Schaffer, N., 2020. Automated detection of rock glaciers using deep learning and object-based image analysis. *Remote Sens. Environ.* 250, 112033 <https://doi.org/10.1016/j.rse.2020.112033>.

Schaffer, N., MacDonell, S., Réveillet, M., Yáñez, E., Valois, R., 2019. Rock glaciers as a water resource in a changing climate in the semiarid Chilean Andes. *Reg. Environ. Chang.* <https://doi.org/10.1007/s10113-018-01459-3>.

Scherler, D., Bookhagen, B., Strecker, M.R., 2011. Spatially variable response of Himalayan glaciers to climate change affected by debris cover. *Nat. Geosci.* 4 (3), 156–159 doi: <http://www.nature.com/ngeo/journal/v4/n3/abs/ngeo1068.html#supplementary-information>.

Schmid, M.O., Baral, P., Gruber, S., Shahi, S., Shrestha, T., Stumm, D., Wester, P., 2015. Assessment of permafrost distribution maps in the Hindu Kush Himalayan region using rock glaciers mapped in Google Earth. *Cryosphere* 9 (6), 2089–2099. <https://doi.org/10.5194/tc-9-2089-2015>.

Scotti, R., Brardinoni, F., Alberti, S., Frattini, P., Crosta, G.B., 2013. A regional inventory of rock glaciers and talus ramparts in the central Italian Alps. *Geomorphology* 186, 136–149. <https://doi.org/10.1016/j.geomorph.2012.12.028>.

Seppi, R., Carton, A., Zumiani, M., Dall'Amico, M., Zampedri, G., Rigon, R., 2012. Inventory, distribution and topographic features of rock glaciers in the southern region of the Eastern Italian Alps (Trentino). *Geogr. Fis. Din. Quat.* 35 (2), 185–197. <https://doi.org/10.4461/GFDQ.2012.35.17>.

Shannon, S., Smith, R., Wiltshire, A., Payne, T., Huss, M., Betts, R., Caesar, J., Koutoulis, A., Jones, D., Harrison, S., 2019. Global glacier volume projections under high-end climate change scenarios. *Cryosphere* 13 (1), 325–350. <https://doi.org/10.5194/tc-13-325-2019>.

Smith, T., Bookhagen, B., 2018. Changes in seasonal snow water equivalent distribution in High Mountain Asia (1987 to 2009). *Sci. Adv.* 4 (1), e1701550 <https://doi.org/10.1126/sciadv.1701550>.

Thayyen, R.J., Gergan, J.T., 2010. Role of glaciers in watershed hydrology: a preliminary study of a “Himalayan catchment”. *Cryosphere* 4 (1), 115–128. <https://doi.org/10.5194/tc-4-115-2010>.

Vermote, E.F., Tanre, D., Deuze, J.L., Herman, M., Morcette, J., 1997. Second simulation of the Satellite Signal in the Solar Spectrum, 6S: an overview. *IEEE Trans. Geosci. Remote Sens.* 35 (3), 675–686. <https://doi.org/10.1109/36.581987>.

Wagner, T., Pleschberger, R., Kainz, S., Ribis, M., Kellerer-Pirkbauer, A., Krainer, K., Philippitsch, R., Winkler, G., 2020. The first consistent inventory of rock glaciers and their hydrological catchments of the Austrian Alps. *Aust. J. Earth Sci.* 113, 1–23. <https://doi.org/10.17738/ajes.2020.0001>.

Wagner, T., Seelig, S., Helfricht, K., Fischer, A., Avian, M., Krainer, K., Winkler, G., 2021. Assessment of liquid and solid water storage in rock glaciers versus glacier ice in the Austrian Alps. *Sc. Total Environ.* 800, 149593.

Wahrhaftig, C., Cox, A., 1959. Rock glaciers in the Alaska Range. *Geol. Soc. Am. Bull.* 70, 383–436.

Whalley, W.B., Martin, H.E., 1992. Rock glaciers: II models and mechanisms. *Prog. Phys. Geogr.* 16 (2), 127–186.

Zhang, F., Thapa, S., Immerzeel, W., Zhang, H., Lutz, A., 2019. Water availability on the Third Pole: a review. *Water Sec.* 7, 100033 <https://doi.org/10.1016/j.wasec.2019.100033>.

Zhang, Q., Jia, N., Xu, H., Yi, C., Wang, N., Zhang, L., 2022. Rock glaciers in the Gangdise Mountains, southern Tibetan Plateau: Morphology and controlling factors. *Catena* 218, 106561.